



Disturbance rejection control based on acceleration projection method for walking robots

Xu-yang WANG[†], Zhao-hong XU, Tian-sheng LÜ

(School of Mechanical Engineering, Shanghai Jiao Tong University, Shanghai 200240, China)

[†]E-mail: wangxuyang@sjtu.edu.cn

Received Apr. 1, 2008; revision accepted June 10, 2008

Abstract: This paper presents a disturbance rejection scheme for walking robots under unknown external forces and moments. The disturbance rejection strategy, which combines the inverse dynamics control with the acceleration projection onto the ZMP (zero moment point)-plane, can ensure the overall dynamic stability of the robot during tracking the pre-computed trajectories. Under normal conditions, i.e., the system is dynamically balanced, a primary inverse dynamics control is utilized. In the case that the system becomes unbalanced due to external disturbances, the acceleration projection control (APC) loop, will be activated to keep the dynamic stability of the walking robot through modifying the input torques. The preliminary experimental results on a robot leg demonstrate that the proposed method can actually make the robot keep a stable motion under unknown external perturbations.

Key words: Inverse dynamics, Disturbance rejection, ZMP (zero moment point)-plane, Orthogonal projection, Walking robot
doi:10.1631/jzus.A0820242 **Document code:** A **CLC number:** TP242.1

INTRODUCTION

Stability maintenance is always regarded as one of the most important topics in the motion control for walking robots. In contrast to other industrial manipulators, the interaction between the walking robots and the ground subjects to unilateral constraints, which makes the robots easily overturn during the motion. Furthermore, the robots have to deal with all kinds of disturbances in the real environment, e.g., the interactions with the external environment or with humans. A loss of stability might result in a potentially disastrous consequence for both robots and human beings. In this sense, the designed controller should possess the capability for disturbance rejection.

Researches related to biped locomotion and stable walking control have been developed rapidly in recent years. Several researchers proposed balancing compensators and compliance controllers for humanoid walking based on zero moment point (ZMP) criteria (Takanishi *et al.*, 1990; Hirai *et al.*, 1998;

Kajita *et al.*, 2001). Takanishi *et al.* (1990) described a control method of dynamic biped walking to compensate for the moment on an arbitrary planned ZMP by trunk motion and studied the corresponding motion control under unknown external forces. According to the preset ZMP trajectory, the trunk motion pattern was calculated to compensate the deviations caused by the external forces. The environment adaptability of the robot was improved with this ZMP compensative motion control. However, this method is based on the preset ZMP trajectories but not the actual ones, which might result in large errors for the deflections between the preset and the actual ZMP. Hirai *et al.* (1998) put forward the concept of tipping moment, which can be calculated according to the distance between the desired ZMP and the center of the actual ground reaction force. To recover the robot posture, the ground reaction force control and model ZMP control were used in their posture recovery control. The center of the actual ground reaction force or ZMP was shifted to an appropriate position by adjusting each foot's desired position and attitude,

whereby the robot could be recovered to a balanced posture.

The ZMP tracking method provides an effective approach for walking motions. However, the stability of the motion is improved at the cost of reducing the motion flexibilities. Presently, more and more researchers intend to combine the ZMP control with other model-based methods (Kajita *et al.*, 2003a; 2003b; Sugihar *et al.*, 2002; Kondak *et al.*, 2003). As one of them, Kondak (2003) proposed a ZMP-plane projection control method, in which the algorithm is based on a decoupling of the non-linear model and steering torques to maintain the stability of the system. As an extension of the ZMP-plane projection method, a disturbance rejection scheme is presented in this paper. This scheme behaves a switching manner between the inverse dynamics control and the ZMP-plane projection method. When the robot becomes unbalanced due to external unexpected disturbances, the input torques can be regulated to account for both the track-followings and the stability of the system.

INVERSE DYNAMICS CONTROL

By applying the Lagrange's equation of motion to a conservative system, the dynamic model of walking robot can be derived as

$$D(q)\ddot{q} + h(q, \dot{q}) + G(q) = \tau, \tag{1}$$

where q is the vector of the generalized coordinates, $D(q)$ is a $n \times n$, symmetric, positive-definite inertia matrix, $h(q, \dot{q})$ is a $n \times 1$, centrifugal vector which contains the centrifugal acceleration and Coriolis terms, $G(q)$ is a $n \times 1$ gravitational vector, and τ is a $n \times 1$ external torque vector.

Given a desired reference trajectory $q_r(\cdot)$, a controller can be designed and implemented. The output of the controller τ_q will drive asymptotically the actual trajectory q and \dot{q} to q_r and \dot{q}_r , respectively.

The design of the controller involves decomposing the control design problem into an inner-loop design and an outer-loop design. The inner-loop is to perform feedback linearization of the robotic system, which depends on the inverse dynamic model of the robot. The computed torque can be written as

$$\tau_q = D(q)\ddot{q}_r + h(q, \dot{q}_r) + G(q). \tag{2}$$

The nonlinearities of the system can be eliminated with Eq.(2). Therefore, by substituting Eq.(2) into Eq.(1), and assuming that $D(q)$ is nonsingular, we obtain

$$\ddot{q} = \ddot{q}_r. \tag{3}$$

In this way, the complicated non-linear system is converted into a linear one. Furthermore, tracking performance can be improved by designing a feedback compensation loop. The PD control rule is used in this paper, that is

$$\tau_q = D(q)(\ddot{q}_r - K_D \dot{e} - K_P e) + h(q, \dot{q}_r) + G(q), \tag{4}$$

where $e = \theta - \theta_d$ is the trajectory tracking error vector, K_D and K_P are constant gain matrixes. Through selecting appropriate values for K_D and K_P , a critically damped closed-loop performance can be acquired. The detailed diagram of the inverse dynamics control is shown in Fig.1.

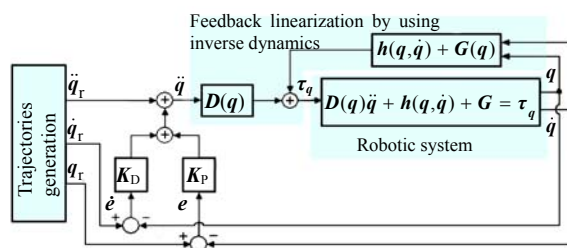


Fig.1 Block diagram of the inverse dynamics control

ZMP AND ZMP-PLANE

The inverse dynamics control works quite well in trajectory-following if we select the appropriate gains for the controller. However, it does not consider the dynamical stability of the walking robot. Walking robot is a dynamically balanced system, and it is easy to overturn during the motion. When large disturbance is applied to the robot, the impacts generated by the disturbance and the compensatory torques will have an influence on the stability. In some circumstances, the robot will become unstable and

overthrow entirely. Thus, in terms of the computed torques, the acceleration $\ddot{\mathbf{q}}$ should be regulated correspondingly to guarantee the dynamics stability of the robot as well as eliminate tracking errors.

ZMP is one of the most famous stability criteria widely used in the biped motion control. Based on the ZMP theory, the ZMP-plane concept is proposed by Kondak (2003) for the biped robot to perform a stable movement. In this paper, the driving torques considering the overall stability can be computed according to the ZMP-plane. The acceleration $\ddot{\mathbf{q}}$ is projected onto a definite ZMP-plane to resist the external disturbance applied to the robot.

ZMP

ZMP is defined as the point on the ground at which the net moment of the inertial forces and the gravity forces has no component along the horizontal axes (Vukobratovic, 2004). Let us consider the locomotion mechanism in the single support phase (Fig.2). The contribution of the part above the ankle is replaced by the force \mathbf{F}_A (F_{Ax} , F_{Ay} , F_{Az}) and the moment \mathbf{M}_A (M_{Ax} , M_{Ay} , M_{Az}). The foot also experiences the ground reaction at point P as well as the gravity $\mathbf{G}=m_f\mathbf{g}$. The ground reaction generally consists of the ground reaction force \mathbf{R} and the moment \mathbf{M} . The horizontal components of the reaction force \mathbf{R} , i.e., R_x and R_y , represent the friction force that is balancing the horizontal component of the force \mathbf{F}_A , whereas the vertical moment M_z represents the resultant moment at point P induced by the friction force.

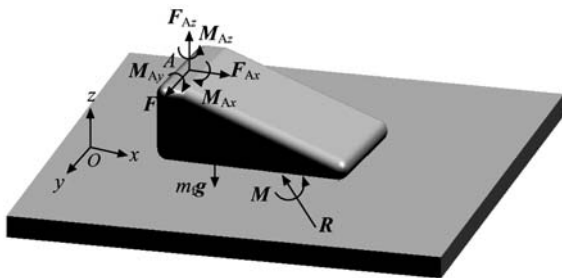


Fig.2 Forces acting on the supporting foot

The static equilibrium equation for the supporting foot can be written as

$$\mathbf{OP} \times \mathbf{R} + \mathbf{OG} \times m_f \mathbf{g} + \mathbf{M}_A + \mathbf{M}_z + \mathbf{OA} \times \mathbf{F}_A = \mathbf{0}, \quad (5)$$

where \mathbf{OP} is a vector from point O to ground reaction point P in Cartesian coordinate, \mathbf{OG} is a vector from

point O to the foot mass center G , \mathbf{OA} is a vector from point O to the ankle joint A , and m_f is the foot mass.

The projection of Eq.(5) onto the horizontal plane yields

$$(\mathbf{OP} \times \mathbf{R})_h + (\mathbf{OG} \times m_f \mathbf{g})_h + (\mathbf{M}_A)_h + (\mathbf{OA} \times \mathbf{F}_A)_h = \mathbf{0}, \quad (6)$$

where h denotes the horizontal y - x plane. Eq.(6) represents the equilibrium equation of the foot, whereby the dynamic stability conditions can be obtained. That is, the position of point P where the ground reaction is acted can be solved from Eq.(6). In this sense, point P is called ZMP. The system is dynamically balanced if the position of point P is within the support polygon.

ZMP-plane

ZMP-plane describes the linearization relationship between the ZMP and the joint accelerations, which can be derived from the primary ZMP equations. According to the ZMP definition, if the coordinate system origin O is shifted to the ground projection of the foot mass center, Eq.(6) can be simplified as

$$(\mathbf{OP} \times \mathbf{R})_h + (\mathbf{M})_h = \mathbf{0}, \quad (7)$$

where $\mathbf{M}=\mathbf{M}_A+\mathbf{OA} \times \mathbf{F}_A$ is the resultant moment of the whole mechanism at point O . Define $\mathbf{M}=[M_x, M_y, M_z]^T$, $\mathbf{R}=[R_x, R_y, R_z]^T$, and $\mathbf{OP}=[x_{ZMP}, y_{ZMP}, 0]^T$, then Eq.(7) can be rewritten as

$$\begin{cases} M_x - R_z y_{ZMP} = 0, \\ M_y + R_z x_{ZMP} = 0. \end{cases} \quad (8)$$

In accordance with the dynamic equations of the robot, M_y and R_z can be represented explicitly as

$$M_y = \alpha_0 + \alpha_1 \ddot{q}_1 + \dots + \alpha_n \ddot{q}_n, \quad (9)$$

$$R_z = \beta_0 + \beta_1 \ddot{q}_1 + \dots + \beta_n \ddot{q}_n, \quad (10)$$

here

$$\alpha_i = \alpha_i(\mathbf{q}, \dot{\mathbf{q}}), \quad i = 0, \dots, n, \quad (11)$$

$$\beta_i = \beta_i(\mathbf{q}, \dot{\mathbf{q}}), \quad i = 0, \dots, n, \quad (12)$$

where $\alpha_0, \dots, \alpha_n$ and β_0, \dots, β_n are non-linear functions of the generalized coordinates \mathbf{q} and generalized

velocities \dot{q} . By substituting Eqs.(9) and (10) into Eq.(8), we obtain

$$x_{ZMP} = -\frac{M_y}{R_z} = -\frac{\alpha_0 + \alpha_1\ddot{q}_1 + \dots + \alpha_n\ddot{q}_n}{\beta_0 + \beta_1\ddot{q}_1 + \dots + \beta_n\ddot{q}_n}. \quad (13)$$

Accordingly, the explicit representation of x_{ZMP} with respect to the acceleration \ddot{q} is acquired. An equivalent expression to Eq.(13) can be obtained as

$$\gamma_n\ddot{q}_n + \dots + \gamma_1\ddot{q}_1 + \gamma_0 = 0, \quad (14)$$

here

$$\gamma_i = \gamma_i(\mathbf{q}, \dot{\mathbf{q}}, x_{ZMP}), \quad i = 0, \dots, n. \quad (15)$$

Therefore, $\gamma_0, \dots, \gamma_n$ are non-linear functions depending on the generalized coordinates \mathbf{q} , generalized velocities $\dot{\mathbf{q}}$ and x -coordinate of ZMP x_{ZMP} . At the moment t , the system accelerations \ddot{q} can be changed arbitrarily by applying corresponding torques τ_q to the joints. In contrast, the changes of velocities \dot{q} and coordinates q correspond to actual accelerations and velocities (double integrator behavior), respectively. Therefore, the coefficients $\gamma_0, \dots, \gamma_n$ at each moment can be considered as constant and the accelerations \ddot{q} as arbitrary values. Obviously, this conclusion is also applicable to y_{ZMP} . Similar to Eq.(14), we can obtain

$$\eta_n\ddot{q}_n + \dots + \eta_1\ddot{q}_1 + \eta_0 = 0, \quad (16)$$

here

$$\eta_i = \eta_i(\mathbf{q}, \dot{\mathbf{q}}, y_{ZMP}), \quad i = 0, \dots, n. \quad (17)$$

For each moment t , Eq.(14) or Eq.(16) describes a plane in the acceleration space. This plane is the ZMP-plane which was proposed by Kondak firstly in 2003 (Kondak *et al.*, 2003). The physical meaning of the ZMP-plane can be described as selecting an acceleration combination $\ddot{q}_1, \dots, \ddot{q}_n$, and the system can move at this moment in such a way that the x or y coordinate of ZMP will be equal to x_{ZMP} or y_{ZMP} .

ACCELERATION PROJECTION ALGORITHM

The acceleration projection algorithm is to pro-

ject the original acceleration vector $\ddot{q} = [\ddot{q}_1, \dots, \ddot{q}_n]$ onto the ZMP-plane, whereby the resulting acceleration vector $\ddot{q}^* = [\ddot{q}_1^*, \dots, \ddot{q}_n^*]$ ensures that the coordinate of ZMP will be equal to the given x_{ZMP} or y_{ZMP} . Diversified ways are available to implement such a projection operation, whereas the ultimate goal is to create the acceleration vector \ddot{q}^* that lies on the ZMP-plane (or intersection determined by both x_{ZMP} and y_{ZMP}). As shown in Fig.3, two different projection methods are illustrated in a 3D acceleration space. In the first method, the original acceleration vector \ddot{q} is changed to \ddot{q}_1^* in a way that its tip lies on the ZMP-plane. In the second method, i.e. an orthogonal projection, the resulting acceleration vector \ddot{q}_2^* is determined by the perpendicular foot (point P) from the end of the original acceleration vector to the ZMP-plane.

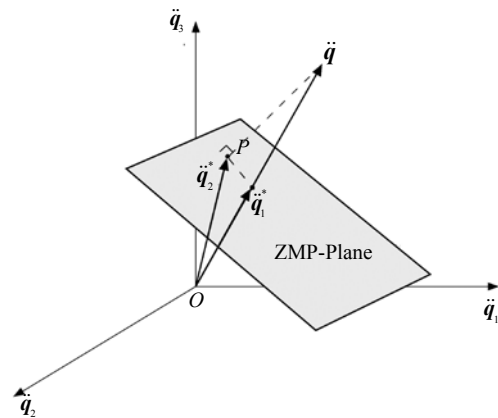


Fig.3 Projection operations in 3D acceleration space

The study has shown that the orthogonal projection leads to the best movement performance among all the others (Kondak *et al.*, 2003). Accordingly, it is adopted in our disturbance rejection controller to acquire a stable movement. Since the perpendicular foot is the nearest point from the original acceleration vector to the ZMP-plane, the resulting acceleration vector \ddot{q}^* can be obtained by solving the minimal distance between the original vector and the ZMP-plane. Let the distance be

$$D(\ddot{q}^*) = \sum_{i=1}^n (\ddot{q}_i^* - \ddot{q}_i)^2, \quad (18)$$

in addition, \ddot{q}^* should satisfy the constraints Φ_1 and Φ_2 , i.e.,

$$\Phi_1(\ddot{q}^*) = \sum_{i=1}^n \gamma_i \ddot{q}_i^* + \gamma_0 = 0, \quad (19)$$

$$\Phi_2(\ddot{q}^*) = \sum_{i=1}^n \eta_i \ddot{q}_i^* + \eta_0 = 0. \quad (20)$$

The minimal distance subject to the constraints Eqs.(19) and (20) can be found by using Lagrange multiplier principle. Correspondingly, the resulting acceleration vector \ddot{q}^* can be also obtained according to

$$\begin{aligned} \frac{\partial D}{\partial \ddot{q}_i^*} + \lambda_1 \frac{\partial \Phi_1}{\partial \ddot{q}_i^*} + \lambda_2 \frac{\partial \Phi_2}{\partial \ddot{q}_i^*} &= 0, \\ \Phi_1 &= 0, \Phi_2 = 0, \quad i = 1, \dots, n, \end{aligned} \quad (21)$$

where λ_1 and λ_2 are Lagrange multipliers.

DISTURBANCE REJECTION CONTROLLER

According to the definition of ZMP-plane, the input acceleration vector \ddot{q} can be revised considering the overall dynamic stability as well as the track-following. As shown in Fig.4, an acceleration projection control (APC) loop is inserted into the inverse dynamics controller. The acceleration projection algorithm is adopted in the APC loop, which makes the original input acceleration vector \ddot{q} be projected onto the ZMP-plane. When the system is dynamically balanced, only the primary inverse dynamics control is used in tracking the predefined trajectories. Once large disturbance is applied or the system becomes unbalanced, the APC loop will be activated to keep the system move in a stable manner.

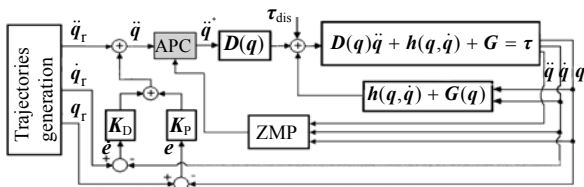


Fig.4 Block diagram of the disturbance rejection controller

To construct an appropriate ZMP-plane is important in the acceleration projection algorithm. When the supporting polygon is rectangle and one edge is parallel to x-axis (and the other is parallel to y-axis), the boundary condition that the system is dynamically balanced is

$$x_{\min} < x_{ZMP} < x_{\max}, \quad y_{\min} < y_{ZMP} < y_{\max}, \quad (22)$$

where x_{\max} and x_{\min} are maximum and minimum boundary of the supporting polygon along the x-axis respectively, y_{\max} and y_{\min} are maximum and minimum boundary of ZMP along the y-axis respectively. The system will become unbalanced if ZMP lies outside of the boundaries. In this case, the ZMP-plane should be placed nearest to the stable zone for the facilities to control. That is, the plane is determined by x_{\max} , x_{\min} or y_{\max} , y_{\min} . The detailed control procedure for the disturbance rejection is shown in Fig.5.

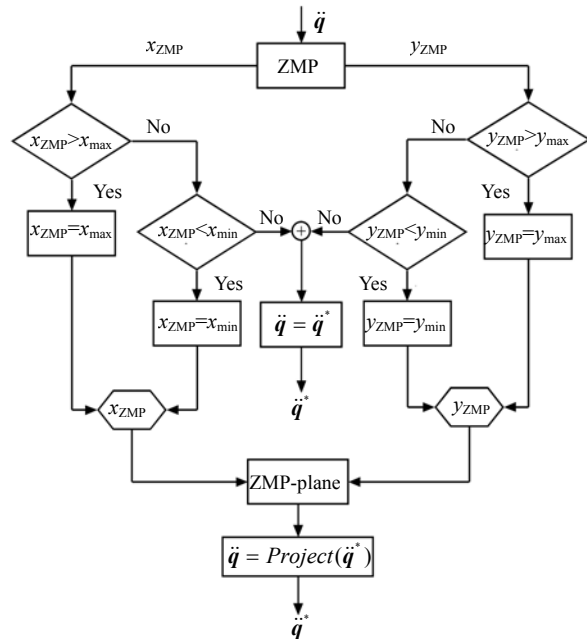


Fig.5 Flowchart of the disturbance control algorithm

SIMULATION EXPERIMENTS

A lot of one-legged systems have been developed during the past few decades. Work on the dynamics and balance of legged systems dates back to Matsouka (1979) and Raibert (1984) making a major contribution to the field. Furthermore, a particular

interest has been expressed in the construction of one-legged robot to simulate the single support phase which appears frequently in the biped walking motion (Pannu *et al.*, 1995; Mitobe *et al.*, 2004). The balance maintenance of one-legged system is a challenge to achieve for its limited support convex, which provides a good platform to test the control algorithm.

To verify the disturbance rejection control law, an experimental one-legged robot is built, as shown in Fig.6. The robot consists of 4 links, i.e., foot, shank, thigh, and waist, and the parameters of the model are given in Table 1. The trunk is modeled as a mass point ($m=0.5036$ kg), whereby the influence of the upper body can be studied. The control algorithm is implemented in Matlab/Simulink environment. The robot is expected to perform a squatting and raising motion. During the motion, disturbances are applied to the robot from different directions. The resulting movement is illustrated in Fig.7, where three pushes with the magnitude of 2 N are acted at points *A* and *B* for 0.125 s, respectively. In detail, the first two pushes occur at point *A* along *x*-axis and the last one happens at point *B* along *y*-axis independently.

Since the contact state is unchanged in the motion, the stability area is fixed as $x_{ZMP} \in [-0.05, 0.1]$

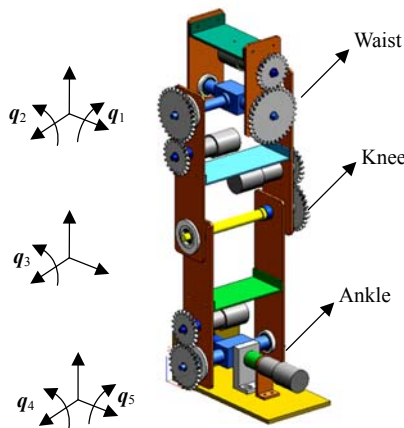


Fig.6 Structural diagram of experimental robot leg

Table 1 Parameters of the robot model

| Link | Length (m) | Mass (kg) |
|-------|------------|-----------|
| Waist | 0.06 | 0.435 |
| Thigh | 0.12 | 0.587 |
| Shank | 0.12 | 0.822 |
| Foot | 0.10 | 0.656 |

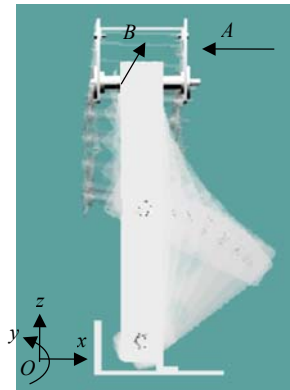


Fig.7 Movement for squatting and raising

and $y_{ZMP} \in [-0.05, 0.05]$ according to the dimensions of the foot ($0.1 \text{ m} \times 0.05 \text{ m}$). Identical servo motors are adopted for the joints, and the driving-torque limits are given as $-2 \text{ N}\cdot\text{m} < \tau_{q_i} < 2 \text{ N}\cdot\text{m}$ ($i=1, \dots, 5$). In the simulations, the gains for Eq.(4) are set as $K_D = [20, 20, 20, 20, 20]^T$ and $K_P = [50, 50, 50, 50, 50]^T$.

The detailed results of the disturbance rejection control are shown in Fig.8, where the dotted and the solid lines represent the reference and the actual trajectories of the joints, respectively. The total simulation time is 10 s and the maximal tracking error happens at 2.5 s, as shown in Fig.9. From Figs.8 and 9, it can be seen that the variations of the trajectories from the reference are very small, which means the tracking control works well even when the system subjects to large external disturbances.

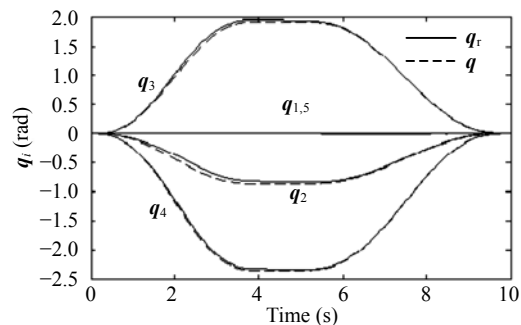


Fig.8 Reference and actual trajectories of the joints

The disturbances and stability of the robot can be illustrated by the ZMP trajectories, as shown in Fig.10. It can be seen that the disturbances denoted as dist 1,

dist 2, and dist 3 are applied to the robot at 2.5, 5.5 and 8.5 s independently. At most of the time, the ZMP lies inside the sole region. Limited by the sampling frequency (1 kHz) and the response time of the motor (0.1 s), some ZMP values exceed the region instantly. Considering that the robot can move at much lower frequency (about several tens of Hertz), instant unstable overstepping can be ignored in the view of the overall stability.

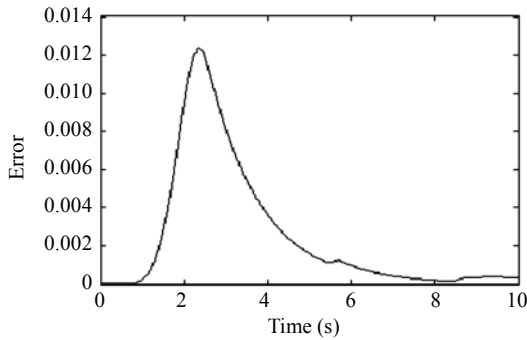


Fig.9 Normalized tracking errors

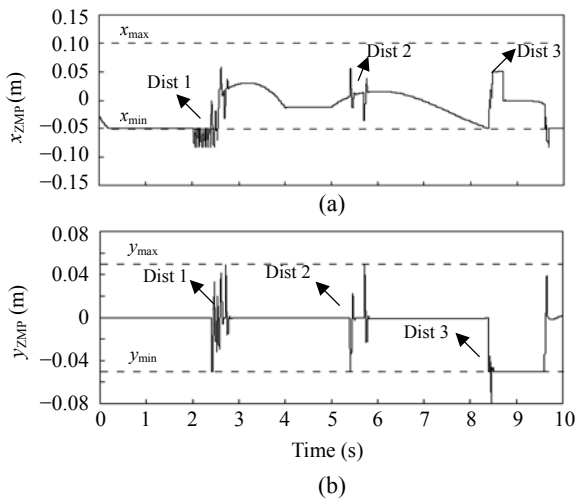


Fig.10 Trajectories for (a) x_{ZMP} and (b) y_{ZMP}

The computed torques are depicted in Fig.11. Corresponding to the ZMP trajectories, we can see that the computed torques are regulated frequently to resist the external disturbances. It should be noticed that the torques generated corresponding to the dist 2 do not result from the APC loop, for the robot is still balanced even under disturbance.

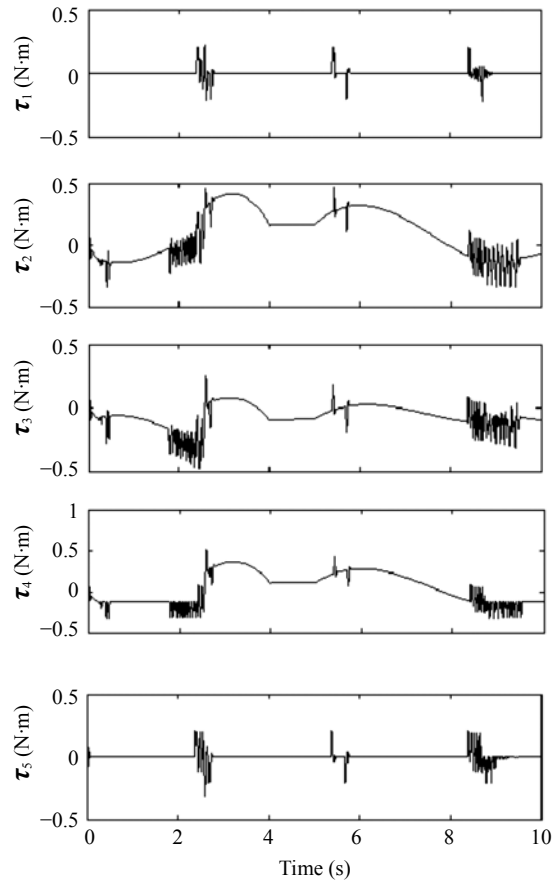


Fig.11 Resulting torques ($\tau_1 \sim \tau_5$) for the joints

CONCLUSION

This paper proposed a disturbance rejection scheme by combining the inverse dynamics control with the acceleration projection algorithm. The controller consists of three parts: (1) an inverse dynamics controller; (2) a PD feedback controller; (3) an acceleration projection controller. The disturbance rejection controller regulates the input torques to realize a stable movement when the robot becomes unbalanced for unexpected disturbances. The simulation results testify the effectiveness of the proposed method. The robot keeps balanced and achieves a good trajectory tracking task even under unknown external perturbations. Our future research will focus on the further experimental study of the disturbance rejection scheme and the application for the real robot platforms.

ACKNOWLEDGEMENT

The authors would like to thank the instruction and support of Dr. Konstantin Kondak, who comes from Technical University of Berlin, Institute for Computer Engineering and Microelectronics, Berlin, Germany.

References

- Hirai, K., Hirose, M., Takenada, T., 1998. The Development of Honda Humanoid Robot. IEEE International Conference on Robotics and Automation, Belgium, p.1321-1326. [doi:10.1109/ROBOT.1998.677288]
- Kajita, S., Yokoi, K., Saigo, M., Tanie, K., 2001. Balancing a Humanoid Robot Using Backdrive Concerned Torque Control and Direct Angular Momentum Feedback. IEEE International Conference on Robotics and Automation, p.3376-3382. [doi:10.1109/ROBOT.2001.933139]
- Kajita, S., Kanehiro, F., Kaneko, K., Fujiwara, K., Harada, K., Yokoi, K., Hirukawa, H., 2003a. Biped Walking Pattern Generation by Using Preview Control of Zero-Moment Point. IEEE International Conference on Robotics and Automation, Taipei, Taiwan, p.1620-1626.
- Kajita, S., Kanehiro, F., Kaneko, K., Fujiwara, K., Harada, K., Yokoi, K., Hirukawa, H., 2003b. Resolved Momentum Control: Humanoid Motion Planning Based on the Linear and Angular Momentum. IEEE/RSJ International Conference on Intelligent Robots and Systems, Las Vegas, USA, p.1644-1650.
- Kondak, K., Hommel, G., 2003. Control and Online Computation of Stable Movement for Biped Robots. IEEE Conference on Intelligent Robots and Systems, Las Vegas, USA, p.874-879. [doi:10.1109/IROS.2003.1250739]
- Matsouka, K., 1979. A Model of Repetitive Hopping Movements in Man. In: Proceedings of the Fifth World Congress on Theory of Machines and Mechanisms. American Society of Mechanical Engineers, New York, p.1168-1171.
- Mitobe, K., Gapi, G., Nasu, Y., 2004. A new control method for walking robots based on angular momentum. *Mechatronics*, **14**:163-174. [doi:10.1016/S0957-4158(03)00028-X]
- Pannu, S., Becker, G., Kazerooni, H., 1995. Stability of a One Legged Robot Using μ -Synthesis. Proceedings of IEEE International Conference on Robotics and Automation, N-agoya, Japan, p.685-690. [doi:10.1109/ROBOT.1995.525363]
- Raibert, M. H., 1984. Hopping in legged systems—modeling and simulation for the two-dimensional one-legged case. *IEEE Transactions on Systems, Man and Cybernetics*, **14**(3):451-463.
- Sugihar, T., Nakamura, Y., Inoue, H., 2002. Realtime Humanoid Motion Generation through ZMP Manipulation Based on Inverted Pendulum Control. IEEE International Conference on Robotics and Automation Washington, DC, p.1404-1409. [doi:10.1109/ROBOT.2002.1014740]
- Takanishi, A., Takeya, T., Karaki, H., Kato, I., 1990. A Control Method for Dynamic Biped Walking under Unknown External Force. Proceedings of IEEE International Workshop on Intelligent Robots and Systems, Ibaraki, Japan, p.795-801. [doi:10.1109/IROS.1990.262498]
- Vukobratovic, M., 2004. Zero-moment point—thirty five years of its life. *International Journal of Humanoid Robotics*, **1**(1):157-173.